

The measurement of G using the MSL torsion balance

M P Fitzgerald and T R Armstrong

Measurement Standards Laboratory (MSL), Industrial Research, PO Box 31-310,
Lower Hutt, New Zealand

Received 22 January 1999, in final form and accepted for publication 4 March 1999

Abstract. This paper describes the improvements that have been made to our measurement of the Newtonian gravitational constant (G) since our last published value of G in 1995. As a result of a new measurement of G made with the improved apparatus, we have discovered some second-order corrections that were omitted from the previous measurement. New values for G are presented; both from the latest measurement and a recalculated value from our previous measurement. Our latest values are $G = 6.6742(7) \times 10^{-11} \text{ m}^3 \text{ kg}^{-1} \text{ s}^{-2}$ for the most recent measurement and $G = 6.6746(10) \times 10^{-11} \text{ m}^3 \text{ kg}^{-1} \text{ s}^{-2}$ for the recalculated 1995 value. These two values agree to within their uncertainties.

Keywords: torsion balance, Newtonian gravitational constant

1. Introduction

The accurate measurement of G , the Newtonian gravitational constant, has proved to be a major challenge to the scientific community. The extent of this challenge has recently been summarized by Gillies [1]. A large part of the difficulty in obtaining a precise value of G is because the gravitational force cannot be screened. This means that the calculation of G from the experimental data requires the evaluation of the gravitational force on all parts of the apparatus. The numerical size of these effects is often similar to or even larger than the uncertainty in the recommended value of G [2] so that errors or omissions can change the value of G significantly.

In 1995, three groups [3–6] published values of G which differed by up to 0.7%. More recent measurements of G [7–10] have produced values that are in agreement to within their quoted uncertainties. However, these new values do not agree with any of the 1995 values.

Following the publication of the MSL result, it was decided to look for any systematic effects in the measurement. A secondary aim was to improve the measurement to obtain a smaller uncertainty in the value of G . To achieve these aims, improvements to the apparatus were made and changes to the mass and dimensions of the test mass were made. A new measurement of G has been carried out after completely realigning and setting up the experiment. During the course of this measurement some second-order corrections that had been omitted from the previous measurement were discovered. These corrections will be described in the following sections.

The preliminary result of our new measurement of G is described in this paper. The first section of the paper describes the measurement method and torsion-balance apparatus developed here at the MSL. The modifications

made to the apparatus are described, together with the effects these changes have had on the experimental signals. The omitted correction factors are then discussed. New values for G are presented; both for the latest measurement and a recalculated value from our 1995 measurement [4].

2. The method

The measurement design has been described in detail previously [3, 4]. Briefly, the measurement method is based on a torsion balance compensated such that the torque produced by the gravitational attraction between the torsion-balance masses is balanced by an electrostatically induced torque. A compensated method was chosen so that the torsion fibre does not twist during the measurement and the suspended mass remains stationary. This was done to reduce the effects of anelastic behaviour of the fibre and the local gravitational gradient on the measurement.

The measurement apparatus is shown in figure 1(a). The torsion balance consists of a small cylindrical mass and mirror suspended from a long slender fibre. Two large cylindrical field masses are used to produce a gravitationally induced torque Γ_G that acts on the suspended cylindrical mass. An autocollimator measures the angular position of the mirror that is attached to the suspended mass. The autocollimator signal is fed to a PID control loop whose output voltage V_G is applied to the electrodes that surround the suspended mass. The control loop adjusts V_G so that the angular position of the mirror and mass system remains constant with respect to the autocollimator and electrodes.

The electrodes and suspended mass form an electrometer. The moving vane of the electrometer is the suspended mass. This avoids the need for extra electrode structures that will additionally load the fibre and complicate the calculation of the gravitational attraction. There are two sides to the

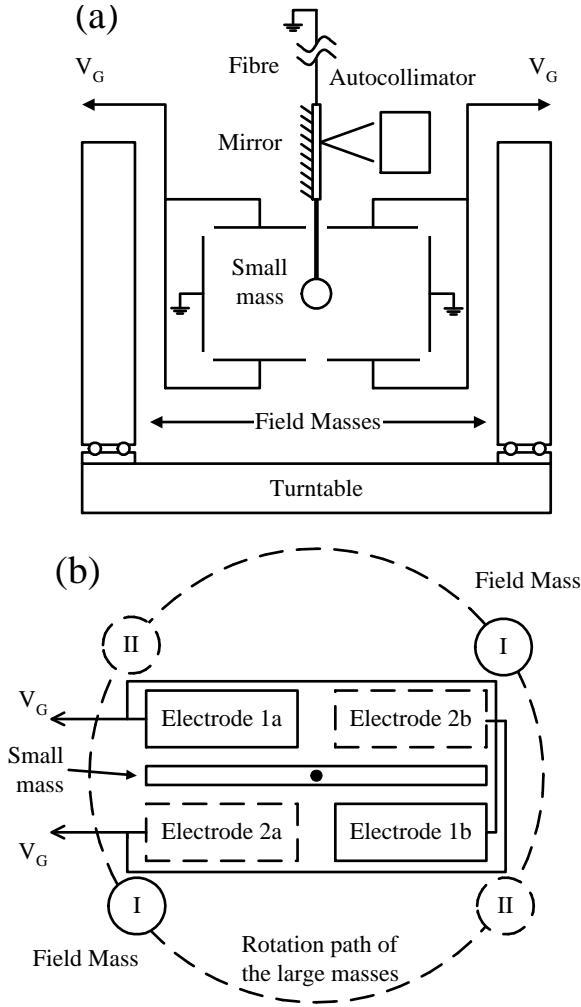


Figure 1. A schematic view of the torsion-balance apparatus and electrometer: (a) a side view and (b) the view from above the apparatus.

electrometer (see figure 1(b)) so that torque can be produced in clockwise and anticlockwise directions. Electrode pairs 1a and 1b are used to produce the clockwise torque while 2a and 2b will produce an anticlockwise torque. The earthed side electrodes (see figure 1(a)) in the electrometer are used to adjust the position of the maximum value of the change in capacitance with the angle $dC/d\theta$ so that it corresponds to the position of the small-mass system.

The two field masses are mounted on a turntable that rotates about the torsion-fibre axis. The control voltage V_G is measured while the masses are positioned at four angular positions for one revolution of the turntable. These positions are where Γ_G is at a maximum with respect to the rotation angle. Γ_G is proportional to V_G^2 so the value of V_G is sampled frequently and squared before being averaged and recorded. Γ_G is related to V_G by

$$\Gamma_G = \frac{1}{2}(dC/d\theta_i)V_G^2 = GK \quad (1)$$

where i refers to the clockwise or anticlockwise side of the electrometer and K is the calculated gravitational torque between the two large masses and the small masses. K is calculated by numerical integration. It includes additional terms such as the gravitational attraction between the small mass and the mounting blocks on which the large masses sit.

The electrometer term $dC/d\theta$ is determined in a separate measurement. This involves measuring the acceleration of the suspended mass when a large voltage V_A is applied to one side of the electrometer. The field masses are removed and the servo loop controlling the position of the suspended mass is turned off. V_A produces a torque that will accelerate the suspended mass towards the energized electrodes. A second control loop is used to control the angular position of the apparatus to ensure that the fibre does not twist. This control loop acts by accelerating the whole torsion balance at the same rate as the suspended mass. The value of $dC/d\theta$ for each side of the electrometer is found from

$$dC/d\theta_i = 2I\ddot{\alpha}/V_A^2 \quad (2)$$

where I is the moment of inertia of the suspended cylinder and mirror system and $\ddot{\alpha}$ is the measured angular acceleration of the torsion balance. V_A is chosen to be larger than V_G so that the acceleration torque can be up to 300 times larger than Γ_G . This significantly reduces the effect of the local gravitational gradient on the measured acceleration.

A value for G is obtained by combining equations (1) and (2) so that

$$G = \frac{1}{2K}(dC/d\theta_i)V_G^2 = (V_G^2/V_A^2)(I/K)\ddot{\alpha}. \quad (3)$$

In practice, the calculation of a single value of G is more complicated. Measurements of V_G must be made with the field mass at two of the angular positions around the fibre axis. This is done to eliminate the rest-point torque of the torsion balance from the calculation. Also the value of V_G^2 must be corrected for the contact potential, V_c , between the copper small-mass system and the stainless steel electrodes in the electrometer.

G is actually calculated from five consecutive positions of the field mass so that the effects of drift in the fibre rest point can be removed. At each mass position V_G is measured using both positive V_{G+} and negative V_{G-} polarity voltages. This allows the calculation of the contact potentials in the electrometer system using

$$V_c = \frac{2\Delta\Gamma_{rest}/(dC/d\theta_i)}{(V_{G+} - V_{G-})} - \frac{1}{2}(V_{G+} + V_{G-}) \quad (4)$$

where $\Delta\Gamma_{rest}$ is the change in the rest-point torque from the time of the V_{G+} measurement to the time of the V_{G-} measurement. The term $\Delta\Gamma_{rest}$ is obtained by taking a linear fit over all the V_G^2 data for each run.

The value for G is then calculated using

$$G = \frac{1}{2K} \left(\frac{1}{4}(V_{G0}^2 + 2V_{G2}^2 + V_{G4}^2) \frac{dC}{d\theta_i} - \frac{1}{2}(V_{G1}^2 + V_{G3}^2) \frac{dC}{d\theta_{i+1}} \right) \quad (5)$$

where $V_{Gn}^2 = \sum[(V_{G+} + V_c)^2 + (V_{G-} + V_c)^2]/(2N)$ and N is the number of points sampled for each polarity.

3. Apparatus

The main experimental details of our apparatus have been described [3, 4]. This section describes the modifications made to the apparatus for the most recent measurements.

Table 1. Apparatus dimensions used in the 1995 and 1997 measurements. The numbers in brackets are the standard uncertainties.

Component	1995 value	1997 value
Cu small mass		
Length (mm)	220.042(3)	219.626(3)
Diameter (mm)	7.929(2)	18.578(2)
Density (kg m^{-3})	8913.8(1)	8913.8(1)
Mass (g)	96.747(1)	531.752(1)
Stainless steel large mass		
Length (mm)	437.80(1)	437.73(1)
Diameter (mm)	101.039(2)	101.036(2)
Density (kg m^{-3})	7947.8(1)	
Mass (g)	27 894.9(1)	27 891.8(1)
Spacing (mm)	435.128(2)	
Angle (rad)	0.953(2)	
W fibre		
Cross section (mm)	$\phi 0.05$	0.3×0.017
Length (mm)	1011	1011
Autocollimator		
Resolution (μrad)		0.2

The cross sectional area of the torsion fibre has been increased. The tungsten torsion fibre used in the previous measurement had a circular cross section with a diameter of $50 \mu\text{m}$. This has been replaced by a tungsten fibre of rectangular cross section of $17 \mu\text{m}$ by $340 \mu\text{m}$ †. This rectangular fibre was chosen to have the same torsional stiffness as the fibre with the circular cross section but it can support three times the load. In addition the fibre loading was increased from 20% to 35% of the fibre yield stress. The new fibre and its higher loading allow the suspended mass to be increased from about 100 g to over 500 g.

The new suspended mass was manufactured by first turning and then grinding a cylinder from a bar of high-purity copper ($>99.99\%$ pure)† using an aluminium oxide grinding wheel. Grinding was chosen to finish the manufacturing of the mass because it produces a cylinder with a better form than that produced by turning and it reduces the risk of contamination from magnetic particles. Samples of the copper ground in the same way as for the small-mass system were then examined using a scanning electron microscope. No evidence of any contamination from the grinding process was observed. The new small-mass system has an average diameter of 18.578 mm which is uniform to within $\pm 0.001 \text{ mm}$.

The orientation of the small mass with respect to the earth's magnetic field was also changed by making the gravitational measurements with the apparatus at a different angular position in the laboratory. The modified and the original dimensions of the apparatus are shown in table 1 together with the standard uncertainties in parentheses, for the significant components.

Several improvements were made to the acceleration method used to measure the $dC/d\theta$ term of the electrometer.

† Both the tungsten fibre and the copper for the small mass system were purchased from Goodfellow Metals Ltd, Cambridge Science Park, Cambridge, UK.

The main change was to increase the number of angular positions measured during each revolution of the apparatus. In the previous measurement an eight-sided polygon and autocollimator system produced eight pulses per revolution. This was increased to 24 pulses per revolution by positioning two additional mirrors near the eight-sided polygon. These mirrors were positioned so that the autocollimator beam can either reflect directly off the face of the polygon or reflect off the polygon, onto one of the extra mirrors and back off the polygon to the autocollimator.

The suspended mass being larger meant that the accelerating torsion balance has a greater response to the gravitational gradient in the laboratory. This gradient is produced by some hills approximately 250 m away from the torsion balance. The gradient is measured by recording the rest point of the torsion balance as a function of its angular position in the laboratory. The additional angular positions available from the polygon and mirrors have increased the resolution of this measurement.

The response of the torsion balance to the local gravitational gradient around the torsion balance has been reduced. This was done by using two large balancing masses. Each mass contains 100 kg of lead shot and is about 600 mm away from the fibre axis. The angular position of each mass is adjusted about the torsion fibre axis so that they approximately balance out the attractions produced by the hills.

The same value of acceleration was used in the current measurement as in the previous measurement [4]. This required an increase in the accelerating voltage from 120 to 270 V.

4. Results and discussion

4.1. Improvements in the gravitational signals

The mass suspended on the new fibre being heavier has increased the measured value of V_G^2 . The measured signal for the 500 g mass is shown in figure 2 together with the signal obtained for the 100 g mass used in the earlier measurement. The increase in the voltage signal is not as large as the factor of five increase in the mass ratio because the suspended mass being of larger diameter has also increased the size of the $dC/d\theta_i$ terms. The measured torques do increase by the same ratio as the masses. For the present measurement the torque was about $7.1 \times 10^{-10} \text{ N m}$ compared with about $1.3 \times 10^{-10} \text{ N m}$ for the previous measurement.

The direction of the applied torque changes each time the large masses are rotated to a new position and this is indicated by the change in the sign of the V_G^2 values. Changing the polarity of the voltage applied to the electrometer causes the small steps in the measurement at each large-mass position. This change of polarity is done to allow the calculation of the contact potential.

The contact potentials associated with the new small-mass system are less than those in the previous measurement. The new small mass used in the measurement was cleaned, measured and immediately installed in the apparatus. The measured contact potentials are about 0.15 V. In contrast, the old small-mass system spent a considerable time in the open

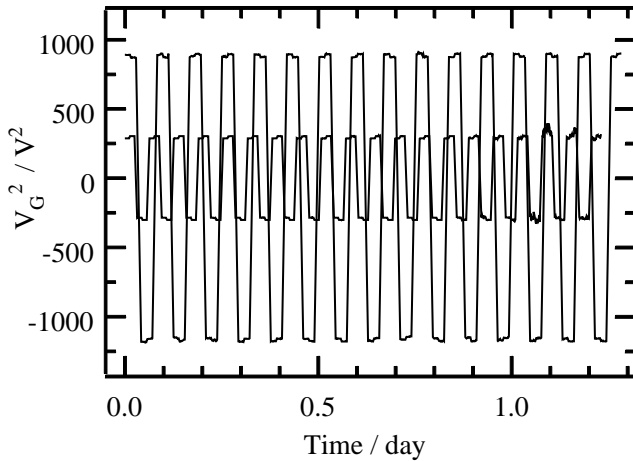


Figure 2. The V_G^2 signals from the 1995 (the central curve) and 1997 measurements. The sign indicates the direction of the applied torque.

air before being maintained under vacuum. In this case, the contact potentials were around 0.25 V.

The measurement times at each position in the two measurements are different. With the larger suspended mass the field masses remained in each location for 40 min. In the earlier measurement, the mass remained stationary for 34 min. These measurement times were chosen to be twice the period of any torque that could be produced by the coupling between the horizontal and the torsion pendulum modes [11] of the torsion balance. The period of this torque is a function of the moment of inertia of the suspended mass and hence of the different measurement periods.

The heavier suspended mass reduced the effect of environmental noise on the measurement of the gravitational torque. The improvement in the noise in the data can be seen in figure 2. For both sets of data shown, the curves start around 3 am on a Sunday and they end around 9 am on a Monday. An increase in the noise for the middle curve at the right-hand end can be seen. This improvement has significantly increased the available measurement time. Previously the noise restricted the data collection to the weekends but now the data can be obtained throughout the week. The greatest improvement has occurred in the acceleration phase of the measurement insofar as these measurements were always performed during the working week when the environmental noise was affecting the measurement. It has also improved the setting up and alignment of the apparatus insofar as this can now be done more quickly instead of waiting a whole week for the results. The reduction in noise is thought to be due to the greater moment of inertia of the heavier suspended mass reducing the angular response of the torsion balance to accelerations caused by seismic noise.

During the course of the latest series of measurements it appeared that the value of G depended upon the rest point of the small-mass system [12]. This effect was not obvious in the 1995 series of measurements because the fibre was more lightly loaded and the drift of the torsion balance rest point was only 0.2 V^2 per day. However, in the current measurement, the rest-point drift changed by around 3 V^2 per day. It turned out that the term to correct for the drift

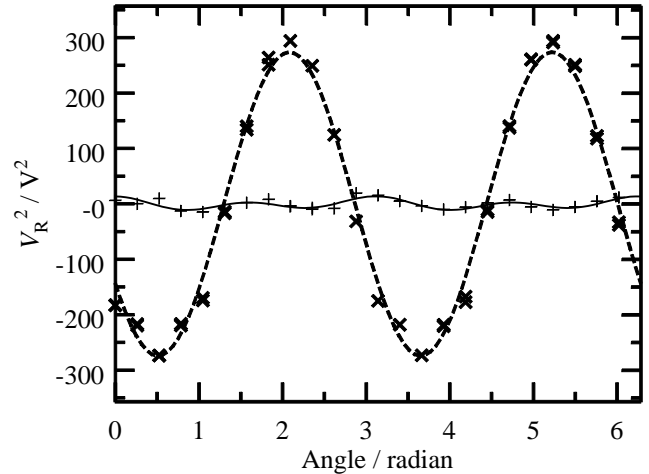


Figure 3. The torsion-balance rest-point voltage V_R^2 as a function of the angular position of the torsion balance in the laboratory, with and without the lead balancing masses.

in the torque had been omitted when calculating the contact potentials. The correct equation is equation (4) that includes the $\Delta\Gamma_{rest}$ term. This correction amounts to a 0.02% shift in the value of G for a 3 V^2 per day rest-point drift.

Another effect discovered during the latest series of measurements was a hardware fault with our high-voltage amplifiers. Careful analysis of the V_G^2 data showed that, when the polarity of the voltage on one side of the electrometer was changed, the high-voltage amplifier exhibited hysteresis. This resulted in a greater settling time for some of the V_G^2 measurements. The data have subsequently been fitted with an exponential correction term in order to correct for this fault. Subsequent measurements with the repaired high-voltage amplifier agreed well with the exponentially corrected data. This correction changes the calculated value of G by 11 ppm for the 1995 measurement and 94 ppm for the latest measurement.

4.2. Improvements in the acceleration measurement

The extra angular positions available during the rotation of the apparatus have allowed us to better characterize the gravitational gradient produced by the hills. Figure 3 shows the measured rest-point voltage squared of the torsion balance V_R^2 as a function of the angular position of the apparatus in the laboratory. The curve drawn with the broken line was obtained without any balancing masses and shows the gravitational gradient of the nearby hill experienced by the torsion balance. The full curve shows the reduced signal obtained when the two lead balancing masses are in place. The torsion fibre is centred on the rotation axis to within $\pm 10 \text{ }\mu\text{m}$ and the apparatus is levelled to within $\pm 20 \text{ }\mu\text{rad}$.

Considerable effort was required to position the lead masses correctly to balance out the effect of the hills. The lead masses have reduced the effect of the gravitational gradient from a peak-to-peak voltage squared of 550 V^2 to 25 V^2 . The size of this residual is close to the best that can be achieved with two balancing masses, because the calculated residual with two masses in the correct position is 20 V^2 peak-to-peak. This reduces the variation in torque experienced by the rotating torsion balance from 0.3 to 0.018%. The effect of

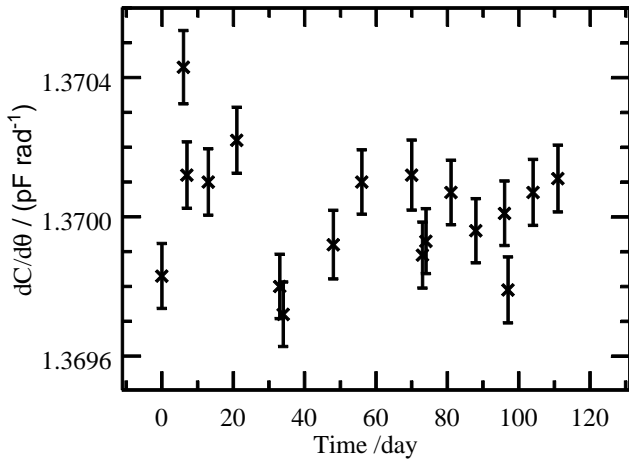


Figure 4. The $dC/d\theta$ term for one side of the electrometer as a function of time. The error bars show both the type A and the type B uncertainty for each measurement.

this varying torque on the electrometer calibration is further reduced by about a factor of ten as it is averaged over two complete rotations. It does not completely cancel out because the torsion balance is accelerating.

Figure 4 shows the results of a series of measurements of $dC/d\theta$ for one side of the electrometer, over a four-month period. The other side of the electrometer gives a similar result but with a different numerical value. The error bars shown in figure 4 correspond to the total uncertainty of each measurement of $dC/d\theta$ of around 70 ppm. The type A uncertainty in each measurement is around 20 ppm. The type B uncertainty in each measurement is around 67 ppm. The comparatively large type B uncertainty occurs because the calculation of $dC/d\theta$ depends both upon the rest-point torque and upon the rate of drift of the rest point of the fibre. Improving our analysis of the data to better calculate these two terms is one area of work required to complete this current series of measurements.

The mean value of $dC/d\theta$ for the data in figure 4 has a standard deviation of 45 ppm. This represents an improvement over the previous measurement [4], for which our final uncertainty in the electrometer calibration was 68 ppm. This 68 ppm uncertainty was achieved only after averaging a much larger number of electrometer measurements. The improvement in the uncertainty is due to the increase in number of angular positions and the lower environmental noise for the larger suspended mass and new fibre.

4.3. The calculation of G

The initial analysis of the measurement using the 500 g mass system produced a value that was 0.4% smaller than the value obtained in 1995 [4]. In an attempt to find the source of this discrepancy, various measurements were carried out to test the correction factors applied. These included making measurements to check the torque due to the mounting blocks and replacing the smaller suspended mass to repeat the conditions of the original measurement.

Another possible source of error that was investigated was a magnetic interaction between the stainless steel field

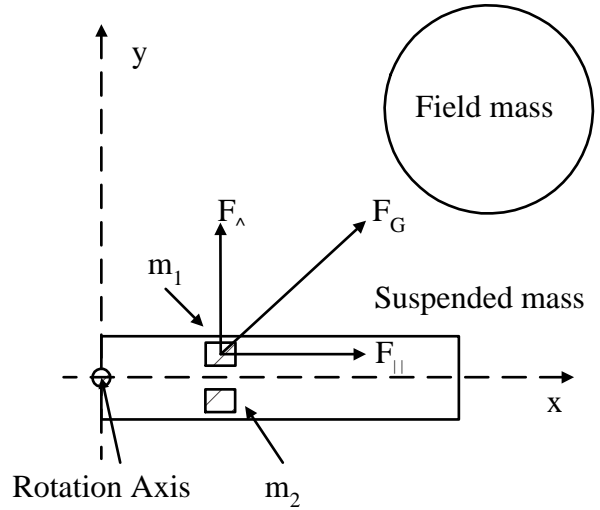


Figure 5. A schematic view showing the components of the gravitational attraction force between one field mass and a small volume of the suspended mass. For clarity only half the suspended mass is shown.

masses and the copper suspended mass. The orientation of the suspended mass was restored to its former orientation with respect to the earth's magnetic field. G was also measured when the horizontal component of the earth's magnetic field was reversed using a set of large Helmholtz coils. In addition, a set of copper field masses was used instead of the stainless steel field masses. Measurements of G were made both with the stainless steel and with the copper masses to check for possible effects produced by the higher magnetic susceptibility of the stainless steel masses. All of these measurements failed to find the source of the disagreement.

The cause of this 0.4% difference was finally traced to an omission of a second-order term in the calculation of the torque between the field mass and the suspended cylinder. The missing term was the torque produced by the component of the gravitational attraction between the suspended mass and the field mass that is parallel to the suspended cylinder axis. This is illustrated in figure 5. The gravitational force of attraction F_G between a small volume of mass m can be resolved into perpendicular F_\perp and parallel components F_\parallel . The torque Γ_m produced by two small masses, m_1 and m_2 , symmetrically positioned about the small-mass axis is given by

$$\Gamma_m = (F_{\perp 1} + F_{\perp 2})x + (F_{\parallel 2} - F_{\parallel 1})y \quad (6)$$

where the indices 1 and 2 refer to the two masses m_1 and m_2 . The two Γ_\parallel terms, when summed over the cylinder, produce a correction to the calculated torque, K , of about 0.1% for the 8 mm diameter, 100 g mass and 0.5% for the 18 mm diameter, 500 g mass. The omission of this Γ_\parallel term accounts for the 0.4% difference between the values of G calculated for the two different suspended masses.

The measured values of G both for the latest series of measurements and for the earlier measurement are shown in figure 6. The G values are plotted as a function of the field-mass position. The locations I and II refer to the field mass positions indicated in figure 1. This is done to average out any density variations in the turntable on which the field masses

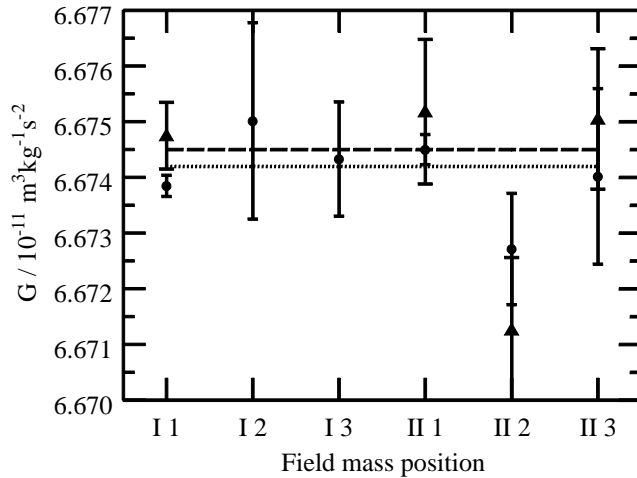


Figure 6. The values of G measured as a function of the large-mass mounting position. I and II are different turntable positions while 1, 2 and 3 indicate the angular positions of the field masses rotated 120° about their axes. ●: 1998 measurements; ▲: 1995 measurements.

are located. Although there appears to be a slight variation between the two positions, the difference is not statistically significant.

The positions 1, 2 and 3 refer to the angular position of each field mass as it is rotated about its axis. These positions are approximately 120° apart. The rotations are done to average out the radial variations in the density of the masses. There was no statistically significant difference among the values of G obtained as the masses were rotated about their axes. This is consistent with the radial density variations previously measured [3].

The values of G for the latest series of measurements were collected over a five-month period in a sequence whereby the mass orientation was changed from 1 to 3 and then back from 3 to 1. The results exhibit no variation with time. This is good confirmation that the fibre drifts have been correctly removed by the data analysis.

The lines in figure 6 indicate the mean values of G obtained. The top line is the recalculated value for the 1995 series of measurements and the lower line is the value for the latest series of measurements. The values represent our current state of knowledge of the measured values of G . Still remaining to be done is a complete uncertainty analysis of our measurement. Our latest values of G are

$$G = 6.6746(10) \times 10^{-11} \text{ m}^3 \text{ kg}^{-1} \text{ s}^{-2}$$

for the 1995 value and

$$G = 6.6742(7) \times 10^{-11} \text{ m}^3 \text{ kg}^{-1} \text{ s}^{-2}$$

or the 1998 value. The uncertainties in the above results are the combination of the type A uncertainty of each measurement and the type B uncertainty used in the 1995 series of measurements [4]. The type A uncertainties are $0.0008 \times 10^{-11} \text{ m}^3 \text{ kg}^{-1} \text{ s}^{-2}$ for the 1995 result and $0.0003 \times 10^{-11} \text{ m}^3 \text{ kg}^{-1} \text{ s}^{-2}$ for the 1998 result. The type B uncertainty used for both measurements is $0.0006 \times 10^{-11} \text{ m}^3 \text{ kg}^{-1} \text{ s}^{-2}$.

5. Conclusion

Repeating the original measurement using a changed apparatus has allowed the identification of several correction terms omitted from the previous measurement. The agreement between the two values of G obtained before and after changes to the apparatus is a good indication that the significant systematic effects have been eliminated. The outcome of this new measurement shows the advantage of making repeat measurements of G with substantial changes to apparatus between each measurement.

Acknowledgments

The authors would like to acknowledge the financial support received from the Marsden Fund administered by the Royal Society of New Zealand and from the Ministry of Research Science and Technology of New Zealand.

References

- [1] Gillies G T 1997 *Rep. Prog. Phys.* **60** 151–225
- [2] Cohen E R and Taylor B N 1987 *Rev. Mod. Phys.* **59** 1121–48
- [3] Fitzgerald M P, Armstrong T R, Hurst R B and Corney A C 1994 *Metrologia* **31** 301–10
- [4] Fitzgerald M P and Armstrong T R 1995 *IEEE Trans. Instrum. Meas.* **44** 494–7
- [5] Wallesch H, Meyer H, Peil H and Schurr J 1995 *IEEE Trans. Instrum. Meas.* **44** 491–3
- [6] Michealis W, Haars H and Augustin R 1995–6 *Metrologia* **32** 267–76
- [7] Bagley C and Luther G G 1997 *Phys. Rev. Lett.* **78** 3047–50
- [8] Cornaz A, Hubler B and Kundig W 1994 *Phys. Rev. Lett.* **72** 1152–5
- [9] Hubler B, Cornaz A and Kundig W 1995 *Phys. Rev. D* **51** 4005–16
- [10] Shurr J, Notling F and Kundig W 1998 *Phys. Rev. Lett.* **80** 1142–5
- [11] Roll P G, Krotkov R and Dicke R H 1964 *Ann. Phys., NY* **26** 442–517
- [12] Armstrong T R and Fitzgerald M P 1996 *CPEM 96 Digest* ed A Braun (IEEE) p 3